Astron. Astrophys. 351, 368–372 (1999)

ASTRONOMY AND ASTROPHYSICS

An unusually intense Ca II K line wing: possible role of particle acceleration in the lower atmosphere

M.D. Ding

Department of Astronomy, Nanjing University, Nanjing 210093, P.R. China (dmd@nju.edu.cn)

Received 16 November 1998 / Accepted 6 August 1999

Abstract. The white-light flare on 1974 October 11 showed an unusual behavior: its Ca II K line reached at flare maximum an intensity of K_1 as high as half of the continuum. This spectral feature cannot be explained by ordinary flare models. We present an abnormal model with an extremely hot temperature minimum region (TMR) that can reproduce the unusually high K_1 intensity. However, this poses a very severe constraint on the energy requirement in the lower atmosphere. Since canonical heating models are insufficient to provide enough heating energy in lower layers, an *in situ* energy source may be required. We further investigate the possible role of a non-thermal particle beam injected from a lower layer. A beam of hecta-keV electrons (or MeV protons) can sufficiently heat the TMR and lead to the formation of a very hot TMR provided that the energy flux of the beam is large enough. Whether such kinds of particle beams exist needs to be checked by more theoretical and observational studies.

Key words: line: profiles – Sun: atmosphere – Sun: flares

1. Introduction

The Ca II K line has been widely used in observations and studies of solar flares. Since it is a collision-dominated line, its radiative temperature, in particular in the line wing, can well reflect the local kinetic temperature of the atmosphere where a line feature originates. There are some semi-empirical models of solar flares based on the Ca II K line (e.g., Machado et al. 1978; Gan & Fang 1987; Ding et al. 1994). Fang et al. (1992) used the line asymmetries of Ca II K to investigate the possible mass motions in lower atmospheric layers.

Recently, Fang et al. (1995) reported an unusual behavior of the Ca II K line in a solar white-light flare (WLF) occurring near the disk center (N12 E02) on 1974 October 11: the intensity of K_1 reached nearly half of the continuum intensity at the flare maximum ($I_\lambda \sim 2.1\ 10^6$ ergs cm^{-2} s^{-1} ster^{-1} Å^{-1}); the intensity of K_3, however, was only weakly increased in comparison. Semi-empirical models, within the general scope of flare models, have been shown unable to reproduce such spectral features (Yin et al. 1995), since the K_1 intensity corresponds to a radiative temperature as high as ~ 5700 K (Fang et al. 1995).

It is well known that the K_1 feature is formed in the temperature minimum region (TMR). Consequently we propose an atmospheric model with an extremely hot TMR that can reproduce the high K_1 intensity. It is nearly impossible to produce such a TMR by canonical energy transport mechanisms in solar flares, where the flare energy is initially released in the corona and then transported downwards through various ways (e.g., particle beam bombardment, heat conduction, and soft X-ray irradiation). Instead, an *in situ* energy source appears to be required.

The purpose of this paper is to compute an atmospheric model for this WLF and to discuss the energy requirement in the lower atmosphere. A possible heating mechanism by high energy particles, injected from a lower layer, is in particular discussed.

2. The flare atmospheric model

So far, several atmospheric models for solar WLFs have been proposed. They can be divided into two groups. The first group includes models with a hot and condensed chromosphere (Avrett et al. 1986) or a chromospheric condensation (Gan et al. 1992). The continuum emission from these models originates mainly from the recombination of hydrogen atoms in the chromosphere and thus shows a distinguishable Balmer or Paschen jump. In comparison, models in the second group exhibit a heated upper photosphere (e.g., Avrett et al. 1986; Mauas et al. 1990; Ding et al. 1994). The continuum emission is then mainly due to the negative hydrogen emission in the upper photosphere. No Balmer or Paschen jump is present in this second case. The above two groups of models correspond to Types I and II WLFs respectively (Machado et al. 1986; Fang & Ding 1995).

For the event of 1974 October 11 discussed here, Fang et al. (1995) stated that it might belong to a Type I WLF, since its radio burst coincided with the maximum of continuum emission and higher Balmer lines appeared. However, the fact that the Balmer jump was very weak implies that it was a complex event showing also some features of a Type II WLF. Simply, we cannot propose a very hot and condensed chromosphere or a very strong chromospheric condensation to account for the con-

Send offprint requests to: M.D. Ding

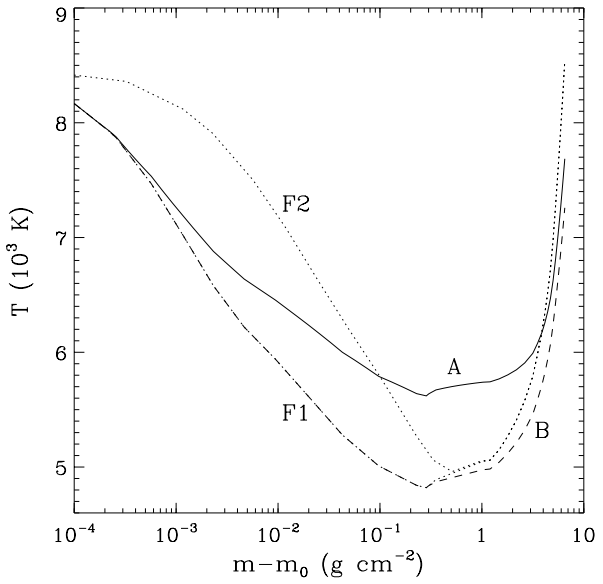

Fig. 1. Temperature distributions for the flare atmospheric models A (solid line) and B (dashed line), corresponding to the times of 03:29:17 and 03:34:21 UT, respectively. The flare models F1 and F2 (dotted lines) of Machado et al. (1980) are also plotted for reference. The coronal column mass densities, m_0, are 3.46 10^{-3} g cm^{-2} for model F2 and 3.14 10^{-4} g cm^{-2} for other models

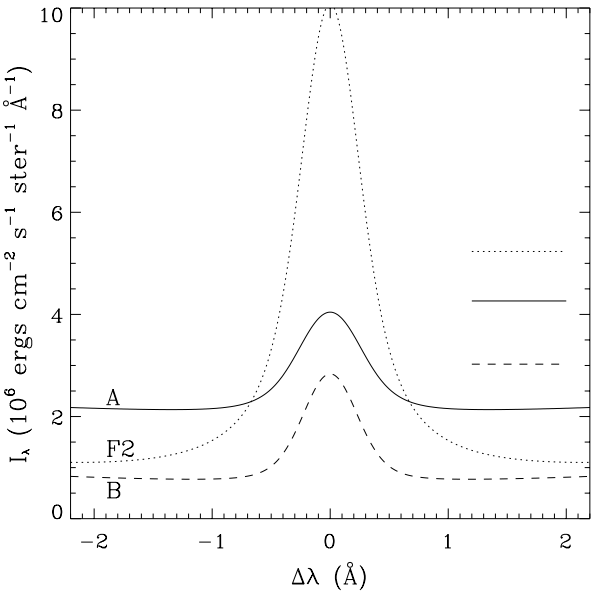

Fig. 2. Ca II K line profiles computed from models A (solid line) and B (dashed line). The profile from model F2 (dotted line) is also given for reference. A Gaussian macro-velocity of 20 km s^{-1} has been used to convolve the profiles. The horizontal lines represent the corresponding continuum intensities at $\lambda = 4000$ Å

tinuum enhancement because it produces a significant Balmer jump that is inconsistent with observations. Therefore, to obtain an atmospheric model for this event, we put our effort mainly in adjusting the temperature structure around the TMR and the upper photosphere, where the K_1 and visible continuum are formed.

Adopting a non-LTE code similar to that used in Ding et al. (1994), we have computed various atmospheric models and obtained by *trial* and *error* a model responsible for the flare emission at 03:29:17 UT, the time when the K_1 and the visible continuum reached their maximum, and a model corresponding to the time of 03:34:21 UT when the K_1 and continuum intensities had decreased substantially (see Figs. 2 and 3 in Fang et al. 1995). Fig. 1 shows the temperature structures for these two models, labeled as A and B, together with the F1 and F2 flare models of Machado et al. (1980). The most interesting thing is, as expected, a very hot TMR in model A. The minimum temperature reaches a value as high as ~ 5620 K, in comparison with the highest value of ~ 5000 K in previous flare models (the F3 model in Avrett et al. 1986). Besides, model A also shows an increased temperature in the upper photosphere relative to model B, which results in a continuum enhancement. Model A shows no more strange behavior than model F1 except for this very hot temperature structure in the TMR.

The Ca II K line profiles computed from models A and B are plotted in Fig. 2, together with the continuum intensities at $\lambda = 4000$ Å. They match the observations fairly well. Since we have not computed the higher Balmer lines (only four bound levels are considered for the hydrogen atom in the present code), there is probably an ununiqueness in the chromospheric structure of these models. However, this does not affect the following discussions on the energy balance in lower layers, provided that the chromosphere is not extremely perturbed, as evidenced in this event.

3. Energetics in the lower atmosphere

The key question that remains to be solved is what mechanism can cause the unusually hot TMR in model A. Canonical heating processes, such as bombardment by energetic particles injected from the corona, irradiation by soft X-rays, or EUV irradiation, seem ineffective to heat the TMR (Machado et al. 1978; Machado & Hénoux 1982; Poland et al. 1988). The chromospheric backwarming effect operates if the chromosphere is hot and condensed enough (Machado et al. 1989), if there is a strong chromospheric condensation (Gan & Mauas 1994), or if the chromosphere is bombarded by an intense particle beam that causes non-thermal excitation and ionization of hydrogen atoms (Aboudarham & Hénoux 1987). All these requisites would also produce a significant Balmer jump in the continuum spectrum which is certainly not the case for the 1974 October 11 event. Therefore, the backwarming mechanism is not relevant either.

Based on these arguments, we suggest that the main energy source lies in the TMR itself, as in the events studied by Mauas et al. (1990) and Ding et al. (1994). Theoretically, magnetic reconnection can occur in lower atmospheric layers (e.g., Li et al. 1997). Although it is still unclear what is the direct consequence of such a reconnection, one may postulate that, high energy particles are accelerated, carrying a significant amount of energy. In the following, we assume that collisional heating

by high energy particles, injected from lower layers, is the main heating source.

3.1. Thermal response of the lower atmosphere due to particle beam heating

To investigate how the very hot TMR is formed, we have to solve the full set of radiation hydrodynamics equations and follow the temporal evolution of the atmosphere. This is a very difficult task at present. In first approximation, we neglect hydrodynamic effects and heat conduction. Then, the energy equation can simply be written as

$$\frac{\mathrm{d}}{\mathrm{d}t}\left[\frac{3}{2}(n_{\rm H}+n_{\rm e})kT+\sum_{i=1}^{N}n_i\varepsilon_i+n_{\rm c}\chi_{\rm H}\right]=H-L+L_0, \quad (1)$$

where n_i and ε_i are the hydrogen level i number density and the corresponding excitation potential, $n_{\rm c}$ is the number density of ionized hydrogen, and $\chi_{\rm H}$ is the ionization potential. Eq. (1) is valid for a pure hydrogen atmosphere. The number of bound levels, N, is taken to be 4. H and L are respectively the collisional heating and radiative cooling rates. L_0 is an extra heating term used to compensate for the radiative cooling in the pre-flare atmosphere, which is assumed not to change during the flare evolution.

The heating rate, due to bombardment by particle beams, can be computed according to formulae given by Emslie (1978). In particular, if the particles are injected from a low layer, we employ a method similar to that in Ding et al. (1998). Assuming a power law for the number flux distribution of the particle beam, we parameterized it by the total energy flux, $\mathcal{F}_1$, the power index, δ, and the low-energy cut-off, E_1. In addition, the particle production site is taken as the middle of the TMR ($m=0.3\,\mathrm{g\,cm^{-2}}$).

The radiative cooling rate is calculated through non-LTE computations. Here, we consider only the lines and continua of H and $\mathrm{H^-}$, which are the main cooling agents in the TMR. When high energy particles are present, the non-thermal excitation and ionization of the hydrogen atoms should be considered in the computations (e.g., Fang et al. 1993). These non-thermal effects raise greatly the local source function, and accordingly change the height distribution of the radiative cooling rate.

Eq. (1) can be solved iteratively together with non-LTE computations of the radiative cooling rate. A more detailed description of this procedure is given in Ding et al. (1999), where the heating due to non-thermal particles in lower layers is used to explain the continuum emission of WLFs. The procedure is summarized as follows. Starting from the pre-flare atmosphere, taken as model B, and injecting a particle beam described as above, the values of H and L are computed at each time step, upon which the atmospheric temperature at the next time step is obtained. This is an explicit procedure which requires that the time interval between successive steps is small enough ($\Delta t\sim 0.01\,\mathrm{s}$). The results indicate that, as long as the particle beam is steady, the whole atmosphere can reach after a certain time ($\sim 20\,\mathrm{s}$) a quasi-stationary state (QSS) in which the radiative cooling is roughly compensated for by the particle beam heating; afterwards, the atmospheric temperature changes very slowly although the particle beam persists.

3.2. Limit of the beam flux due to return current instability

A beam of charged particles generates a return current which can excite instabilities if the drift velocity of the return current exceeds some critical value (Hoyng et al. 1978). For electron beams with a power law distribution, Aboudarham & Hénoux (1986) deduced a formula for the critical energy flux below which the return current is stable against excitation of ion-acoustic or electrostatic ion-cyclotron waves,

$$\mathcal{F}_1^{\rm c}\approx 0.47\sqrt{\frac{kT}{m_{\rm e}}}\frac{\delta-1}{\delta-2}E_1 n_{\rm e}, \quad (2)$$

in the case that ambient electrons and protons have a same temperature. According to Eq. (2), Aboudarham & Hénoux (1986) found that in the coronal environment, electron beams with $\delta=4$ and $E_1=20\,\mathrm{keV}$ are stable when $\mathcal{F}_1\le\mathcal{F}_1^{\rm c}\approx 10^{12}\,\mathrm{ergs\,cm^{-2}\,s^{-1}}$. Apparently, $\mathcal{F}_1^{\rm c}$ is proportional to $n_{\rm e}$, the ambient electron density. In the TMR, $n_{\rm e}$ depends in turn on the energy flux of the particle beam owing to the non-thermal ionization effect. Thus, Eq. (2) becomes implicit and we can only solve it iteratively together with Eq. (1).

Without considering the non-thermal ionization effect, the electron density is only $1.3\ 10^{12}\,\mathrm{cm^{-3}}$ at $m=0.3\,\mathrm{g\,cm^{-2}}$ in the pre-flare atmosphere. However, considering the non-thermal effect leads to a significant increase of the hydrogen ionization degree, which, in turn, raises the value of $\mathcal{F}_1^{\rm c}$. For an electron beam with $\delta=4$ and $E_1=20\,\mathrm{keV}$, $\mathcal{F}_1^{\rm c}$ is computed to be as high as $\sim 3\ 10^{15}\,\mathrm{ergs\,cm^{-2}\,s^{-1}}$ at $m=0.3\,\mathrm{g\,cm^{-2}}$. In fact, such a strong electron beam can result in an electron density at the particle injection site of $\sim 4.5\ 10^{15}\,\mathrm{cm^{-3}}$, three orders of magnitude larger than that in the case without non-thermal ionization effect.

3.3. Possible electron beams responsible for the very hot TMR

We have computed several cases for electron beam heating and obtained the respective QSSs. Fig. 3 plots the results for six cases. We see the effect of varying the low-energy cut-off in the top row and the effect of varying the energy flux in the bottom row, respectively. The average temperature around the TMR is found to increase with increasing E_1. This fact is conceivable. Particles of a higher energy deposit energy over a broader region; meanwhile, the line source function there is enhanced owing to the non-thermal excitation and ionization effect, leading to a stronger radiation field that helps more effectively to heat the particle-free region. The results show that, the QSS in the case where $\mathcal{F}_1=10^{14}\,\mathrm{ergs\,cm^{-2}\,s^{-1}}$, $\delta=4$, and $E_1=100\,\mathrm{keV}$ roughly matches model A in the TMR, and that it leads to a Ca II K line profile and a continuum intensity comparable to observations (Fang et al. 1995). On the other hand, we can also raise the heating effect by purely increasing the energy flux. However, if a smaller E_1 (say, 20 keV) is adopted, a very large $\mathcal{F}_1$, even approaching the critical value as discussed above, would

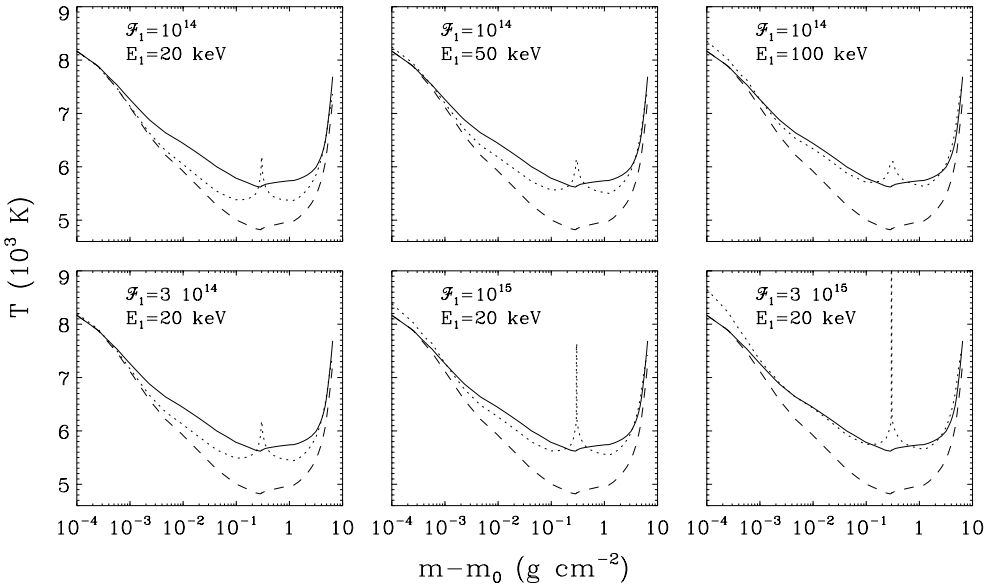

Fig. 3. Temperature distribution (dotted line) for the atmosphere at the quasi-stationary state in the presence of an electron beam heating. The six panels refer to six cases with beam parameters $\mathcal{F}_1$ (in units of ergs cm^{-2} s^{-1}) and E_1 labeled in each panel. In all cases, the power index δ is fixed to be 4. Note that the temperature spikes at the electron production site are somewhat computational artifacts since we have neglected the thermal conduction and the hydrodynamic effect. Models A (solid line) and B (dashed line) are also plotted for reference. See text for details

be needed to yield a QSS comparable to model A. Therefore, such a case is less plausible.

To check further the energetics in the lower atmosphere, we plot in Fig. 4 the column mass distribution of the energy deposition rate, H, by an electron beam and that of the net radiative cooling rate, $L-L_0$, at the very beginning of electron bombardment. An electron beam with $\mathcal{F}_1 = 10^{14}$ ergs cm^{-2} s^{-1} and $E_1 = 100$ keV is adopted which corresponds to the top-right panel in Fig. 3. As expected, there is initially a significant imbalance between the collisional heating and the radiative cooling, implying a net heating effect of the atmosphere. Just around the electron injection site, the energy deposited by beam electrons is obviously the dominant heating energy. However, this energy decreases rapidly with the column mass from the electron injection site. On the other hand, one can find from Fig. 4 that the radiative cooling rate becomes negative in the photosphere, which amounts to $\sim -4\ 10^3$ ergs cm^{-3} s^{-1} at around $m \approx 5$ g cm^{-2}. This means that radiative heating comes into effect and may be comparable to the effect of collisional heating in some particular layers. This negative radiative cooling is caused by an absorption of enhanced radiation from the beam heated layers, within which the non-thermal excitation and ionization effect by beam particles plays a chief role. With the atmosphere being heated, one may expect that the imbalance between the collisional heating and the radiative cooling becomes smaller and it nearly diminishes when the QSS is reached.

Fig. 3 implies that a beam of hecta-keV electrons is a viable candidate responsible for the production of the very hot TMR. Moreover, a fairly large energy flux is needed if the electron beam is the only energy source. Of course, the presence of other heating sources will loose such a stringent requirement.

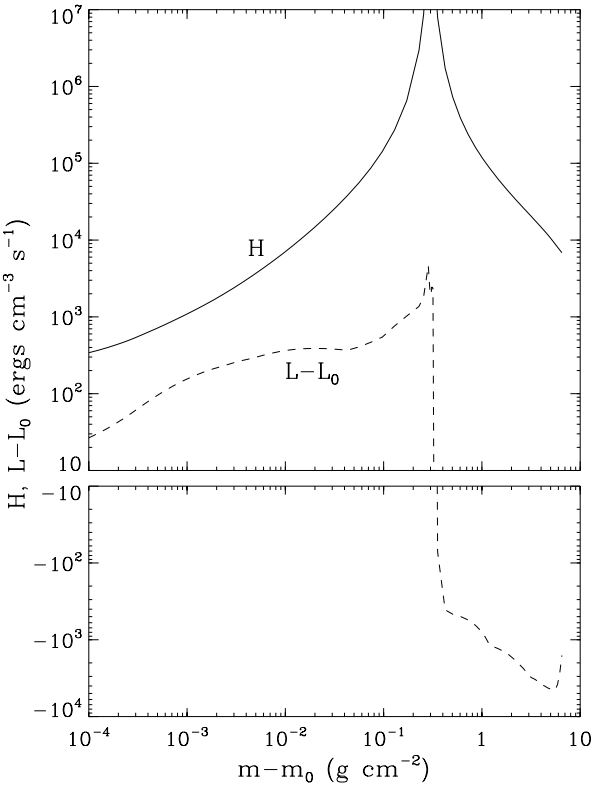

Fig. 4. Rate of energy deposition by an electron beam (solid line), characterized by $\mathcal{F}_1 = 10^{14}$ ergs cm^{-2} s^{-1} and $E_1 = 100$ keV, and net radiative cooling rate (dashed line) computed at the very beginning of electron bombardment

3.4. The role of proton beams

Protons of a given energy cross much shorter column depth than electrons of the same energy. According to Emslie et al. (1996), protons of an energy $\sqrt{m_{\rm p}/m_{\rm e}}$ times that of electrons are required in order to deposit energy over a difference in column mass the same as that for electrons. Therefore, one can expect that the heating results produced by 20, 50, and 100 keV electrons can be alternatively produced by 0.8, 2, and 4 MeV protons, respectively, if the total energy flux remains the same for

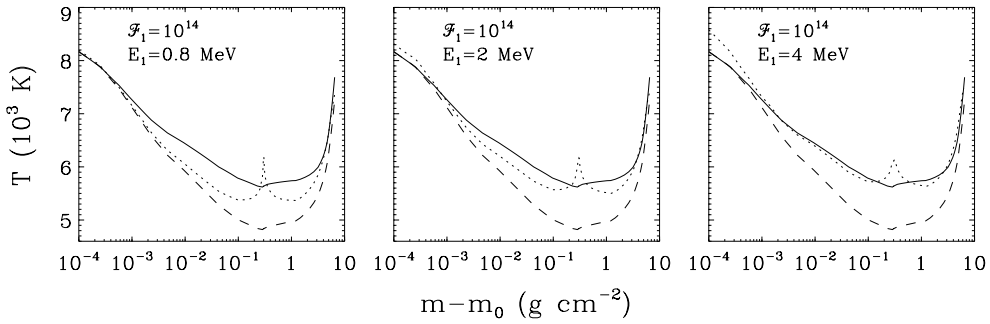

Fig. 5. Temperature distribution (dotted line) for the atmosphere at the quasi-stationary state in the presence of a proton beam heating. The three panels refer to three cases with beam parameters $\mathcal{F}_1$ (in units of ergs cm^{-2} s^{-1}) and E_1 labeled in each panel. In all cases, the power index δ is fixed to be 4. Models A (solid line) and B (dashed line) are also plotted for reference

both particles. For further confirmation, Fig. 5 plots the temperature distributions for the heated atmosphere in the three protons cases, showing a nice correspondence to the three electron cases plotted in the top row of Fig. 3.

4. Conclusions

The white-light flare on 1974 October 11 showed an unusual behavior since at flare maximum Ca II K line reached an intensity of K_1 as high as half of the continuum intensity (Fang et al. 1995). Ordinary flare atmospheric models cannot reproduce such a spectral feature. A model having an extremely hot TMR, with a minimum temperature as high as ~ 5620 K, can explain the unusual Ca II K line but encounters the difficulty in meeting the energy deposit requirement in the lower atmosphere. Pure canonical heating models that transport energy from the corona to lower layers can hardly account for the production of this hot TMR. Therefore, we assume instead an *in situ* energy source. We further investigate the possible role of a particle beam injected from the TMR. The results show that a beam of hecta-keV electrons (or MeV protons) can sufficiently heat the TMR and lead to the formation of the very hot TMR provided that the energy flux of the beam is large enough.

We note that the present study does not rule out other possibilities that produce a hot TMR. In fact, it is very likely that other factors, including even some canonical heating mechanisms, may work together in this event. Theoretical studies of the flare processes in the lower atmosphere, such as magnetic reconnection, particle acceleration, and so on, can help to check what heating sources are plausible.

On the other hand, diagnostics of energetic particles rely on observations of hard X-ray emission or γ-ray line emission. In particular, images at these wavelengths (say, that for hard X-rays) can be used to determine the height of particle acceleration. In the above computations, we have adopted a very large energy flux for the particle beam; however, the volume within which the particles are accelerated is assumed to be small, thus making the observed hard X-ray (γ-ray) emission flux not unrealistically large. Moreover, it is also possible that some of the particles propagating upwards finally escape into the space. For an electron beam with $\delta = 4$ and $E_1 = 100$ keV at $m = 0.3\,\mathrm{g\,cm^{-2}}$, the particle number flux is attenuated to only less than 1% of the initial value when the beam reaches the corona. Thus, the particle flux which could be detected in interplanetary space may still be within the range of values for ordinary solar flares.

Acknowledgements. The author would like to thank an anonymous referee for his/her constructive comments that helped to improve the paper significantly. This work was supported in part by a grant from the Panden Project and a grant from the National Natural Science Foundation of China.

References

Aboudarham J., Hénoux J.-C., 1986, A&A 168, 301
Aboudarham J., Hénoux J.-C., 1987, A&A 174, 270
Avrett E.H., Machado M.E., Kurucz R.L., 1986, In: Neidig D.F. (ed.) The Lower Atmosphere of Solar Flares. National Solar Observatory, Sunspot, NM, p. 216
Ding M.D., Fang C., Gan W.Q., Okamoto T., 1994, ApJ 429, 890
Ding M.D., Fang C., Yun H.S., 1999, ApJ 512, 454
Ding M.D., Hénoux J.-C., Fang C., 1998, A&A 332, 761
Emslie A.G., 1978, ApJ 224, 241
Emslie A.G., Hénoux J.-C., Mariska J.T., Newton E.K., 1996, ApJ 470, L131
Fang C., Ding M.D., 1995, A&AS 110, 99
Fang C., Hénoux J.-C., Gan W.Q., 1993, A&A 274, 917
Fang C., Hiei E., Yin S.Y., Gan W.Q., 1992, PASJ 44, 63
Fang C., Yin S.Y., Hiei E., Ding M.D., Fu Q.J., 1995, Solar Physics 158, 387
Gan W.Q., Fang C., 1987, Solar Phys. 107, 311
Gan W.Q., Mauas P.J.D., 1994, ApJ 430, 891
Gan W.Q., Rieger E., Zhang H.Q., Fang C., 1992, ApJ 397, 694
Hoyng P., Knight J.W., Spicer D.S., 1978, Solar Phys. 58, 139
Li X.Q., Song M.T., Hu F.M., Fang C., 1997, A&A 320, 300
Machado M.E., Avrett E.H., Falciani R., et al., 1986, In: Neidig D.F. (ed.) The Lower Atmosphere of Solar Flares. National Solar Observatory, Sunspot, NM, p. 483
Machado M.E., Avrett E.H., Vernazza J.E., Noyes R.W., 1980, ApJ 242, 336
Machado M.E., Emslie A.G., Avrett E.H., 1989, Solar Phys. 124, 303
Machado M.E., Emslie A.G., Brown J.C., 1978, Solar Phys. 58, 363
Machado M.E., Hénoux J.-C., 1982, A&A 108, 61
Mauas P.J.D., Machado M.E., Avrett E.H., 1990, ApJ 360, 715
Poland A.I., Milkey R.W., Thompson W.T., 1988, Solar Phys. 115, 277
Yin S.Y., Fang C., Ding M.D., Hiei E., Fu Q.J., 1995, Acta Astron. Sin. 36, 279